

Emission line diagnostics for a coronal condensation

P. K. Raju *Indian Institute of Astrophysics, Bangalore 560 034*

Received 1989 January 17; accepted 1989 May 4

Abstract. Theoretical line emission rates for the coronal ions Fe x, Fe xi, Fe xiii, Fe xiv, Ca xii, Ca xiii, and Ca xv, have been used to obtain various line intensity ratios as a function of electron density and electron temperature. The lines are due to the forbidden transitions in the visible part of the spectrum. With the help of these theoretical line intensity ratios physical parameters for a coronal condensation observed during the eclipse of 1965 May 30 have been derived. A simple model consisting of two regions of equal path length one at temperature of $1.25 \times 10^6\text{K}$ and the other at $2.5 \times 10^6\text{K}$ and with constant electron density of $5 \times 10^8 \text{cm}^{-3}$ seems to explain the observed intensities. The analysis also indicates that the observed Ca xiii line intensity appears to be high by about a factor of 4.

Key words : emission line diagnostics—coronal condensations

1. Introduction

Solar corona exhibits a very rich spectrum at visible wavelengths. The quantitative interpretation of such a spectrum is a difficult task. This is mainly due to the vast amount of reliable atomic data required to obtain emission rates. Mason (1975) has considered in detail the excitation of forbidden lines for the coronal ions Fe x, Fe xi, Fe xiv, Ca xii, Ca xiii and Ca xv. The lines are in the visible part of the spectrum. Mason has tabulated emission rates for these lines for several electron densities and electron temperatures. We have used these emission rates to obtain various line intensity ratios. For Fe xiii ion we have considered the line intensity ratios obtained by Flower & Pineau des Forêts (1973). With the help of the theoretical line intensity ratios we have tried to infer the values of electron density and temperature within a coronal condensation observed during the eclipse of 1965 May 30. The observed line intensities are listed by de Boer *et al.* (1972)

2. Line intensity ratios

The theoretical emission rates tabulated by Mason (1975) have been used to obtain the following line intensity ratios :

$I(\text{Ca xv}^a)/I(\text{Ca xiii})$; $I(\text{Ca xv}^a)/I(\text{Ca xii})$; $I(\text{Ca xv}^a)/I(\text{Ca xv}^b)$; $I(\text{Ca xv}^b)/I(\text{Ca xiii})$; $I(\text{Ca xv}^b)/I(\text{Ca xii})$; $I(\text{Ca xiii})/I(\text{Ca xii})$; $I(\text{Ca xiii})/I(\text{Fe xiv})$; $I(\text{Ca xii})/I(\text{Fe xiv})$; $I(\text{Ca xv}^a)/I(\text{Fe xiv})$; $I(\text{Ca xv}^b)/I(\text{Fe xiv})$; $I(\text{Ca xiii})/I(\text{Fe x})$; $I(\text{Ca xii})/I(\text{Fe x})$; $I(\text{Ca xiii})/I(\text{Fe xi}^a)$; $I(\text{Ca xiii})/I(\text{Fe xi}^b)$; $I(\text{Ca xii})/I(\text{Fe xi}^a)$; $I(\text{Ca xii})/I(\text{Fe xi}^b)$; $I(\text{Fe xi}^a)/I(\text{Fe xiv})$; $I(\text{Fe xi}^b)/I(\text{Fe xiv})$; $I(\text{Fe x})/I(\text{Fe xiv})$; $I(\text{Fe xi}^a)/I(\text{Fe x})$; $I(\text{Fe xi}^b)/I(\text{Fe x})$; $I(\text{Fe xiii}^a)/I(\text{Fe xiii}^b)$; $I(\text{Fe xiii}^b)/I(\text{Fe xiii}^c)$; $I(\text{Fe xi}^a)/I(\text{Fe xi}^b)$.

The observed lines with their wavelengths and intensities are listed in table 1. The variation of the several line intensity ratios with electron density and temperature are shown in figures 1 to 12. The temperature values in units of 10^6 K are indicated on each curve. The intensity ratios of lines belonging to dissimilar elements are sensitive to temperature variations. This is because equilibrium ion densities are strongly temperature dependent (Landini & Fossi 1972). Since we are dealing with lines in the visible part of the spectrum the intensity ratios for lines of a given ion would be insensitive to temperature for the temperature range considered in this investigation. Such line intensity ratios would be solely dependent on electron density.

Table 1. Observed line intensities (de Boer *et al.* 1972)

Ion	Wavelength Å	Line intensity‡ (erg cm ⁻² s ⁻¹ sterad ⁻¹)
Ca xii	3327	0.36
Ca xiii	4088	1.65
Ca xv ^a	5694	0.21
Ca xv ^b	5444	—
Fe x	6374	60.4
Fe xi ^a	3986	4.05
Fe xi ^b	7892	—
Fe xiii ^a	3388	16.1
Fe xiii ^b	10747	—
Fe xiii ^c	10797	—
Fe xiv	5303	54.9

‡Line intensities refer to the location on the sun at $\rho = 1.02$.

The electron density dependence of the various line intensity ratios can be understood in the following manner. The spectral lines under consideration are due to the transitions among the metastable levels of the ground term for each ion. For such transitions the spontaneous radiative probabilities are small and comparable to electron collisional rates for coronal electron densities. These comparable transition rates would make the level populations within the ground term to be dependent on electron density. Since line emissivity is proportional to the upper level populations emission rate would be a function of electron density. Thus, intensity ratio of two spectral lines would also be electron density dependent.

For the sake of illustration let us consider the intensity ratio $I(\text{Ca xv}^b)/I(\text{Ca xiii})$. Examining the ground term level population for these two ions (Mason 1975), we

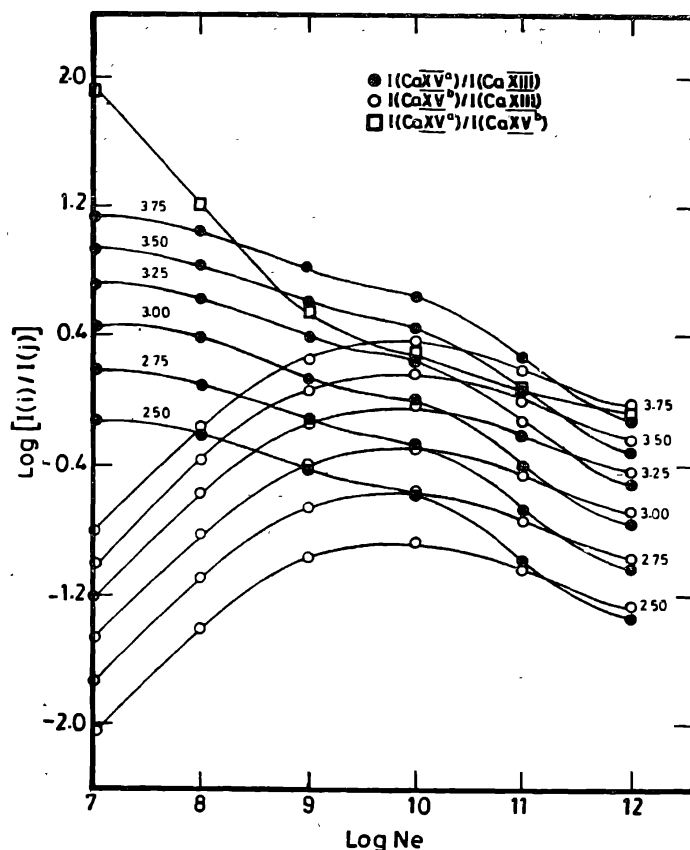


Figure 1. Intensity ratios $I(i)/I(j)$ as a function of N_e , the electron density. The numbers on each curve represents the electron temperature in units of 10^6 K. The spectral line is represented by ion responsible for it. Corresponding wavelengths are shown in table 1.

find that the upper level of the transition for the Ca xv^b line increases with electron density faster than that for Ca xiii line till about electron density of about 10^{10} cm⁻³. Thereafter the trend reverses. This trend is reflected for the intensity ratio $I(\text{Ca xv}^b)/I(\text{Ca xiii})$ in figure 1. In the case of the intensity ratio $I(\text{Ca xiii})/I(\text{Fe xiv})$ the upper level for the Fe xiv line increases faster than that for the Ca xiii line till about the electron density of 10^9 cm⁻³ and the trend reverses thereafter. This behaviour is reflected for the intensity ratio $I(\text{Ca xiii})/I(\text{Fe xiv})$ in figure 4. In a similar manner variation with electron density of other intensity ratios in figures 1 to 12 can be understood.

3. Physical parameters for a coronal condensation and discussion

In this section we use the theoretical intensity ratios to obtain the values of the physical parameters responsible for line radiations in an observed coronal condensation. The coronal condensation considered here was observed during the eclipse of 1965 May 30 (de Boer *et al.* 1972). For sake of simplicity the condensation is assumed to have cylindrical structure and electron density constant within the

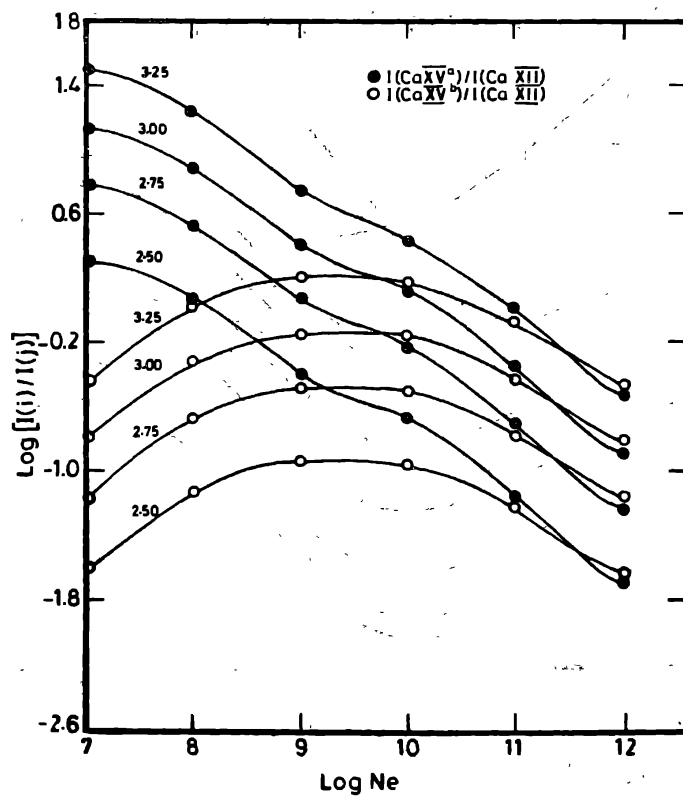


Figure 2. Same as for figure 1.

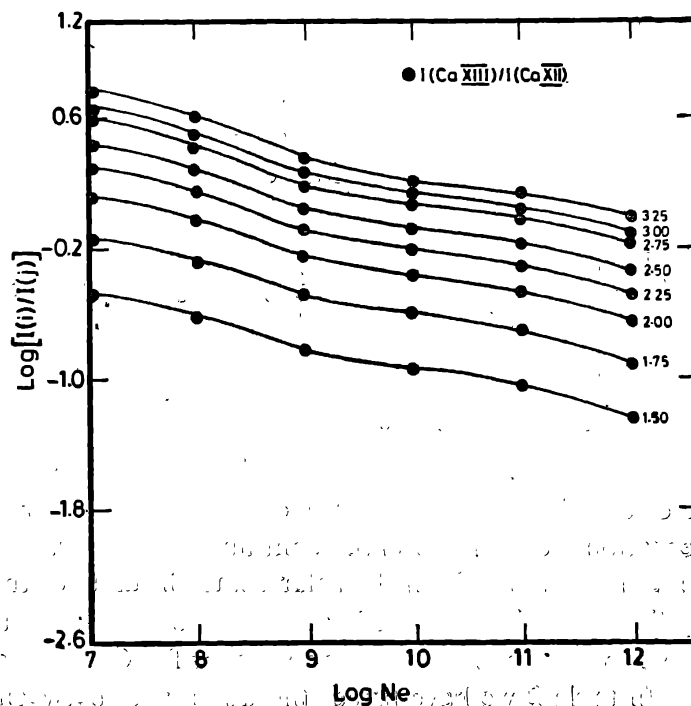


Figure 3. Same as for figure 1.

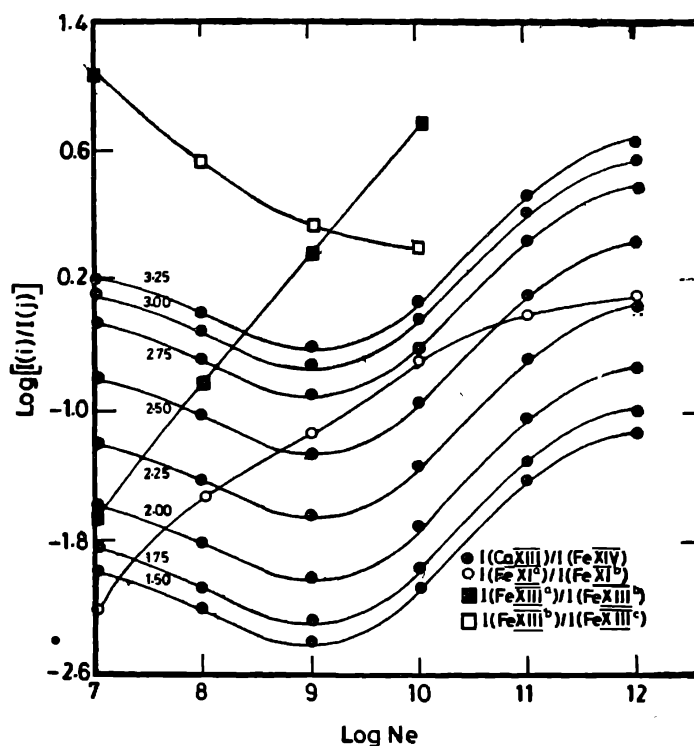


Figure 4. Same as for figure 1.

short path length of the condensation along the line of sight. The ions considered are dominant emitters covering a wide temperature range (1.0 to 3.0×10^6 K). It would be appropriate to consider a distribution of temperatures to explain the entire set of observed lines from the coronal condensation. To facilitate discussion we consider the condensation to consist of two temperature zones of equal path length : one region having low electron temperature value and the other being at 2.5×10^6 K. We consider the following four combinations for the physical parameters :

- | | | |
|---|---|---|
| (i) $T_e = 1.0 \times 10^6$ K and 2.5×10^6 K | } | $N_e = 5 \times 10^8 \text{ cm}^{-3}$ |
| (ii) $T_e = 1.25 \times 10^6$ K and 2.5×10^6 K | | |
| (iii) $T_e = 1.0 \times 10^6$ K and 2.5×10^6 K | } | $N_e = 7.5 \times 10^8 \text{ cm}^{-3}$ |
| (iv) $T_e = 1.25 \times 10^6$ K and 2.5×10^6 K | | |

T_e is the electron temperature. N_e is the electron density and the values chosen are close to the value of $6 \times 10^8 \text{ cm}^{-3}$, which was obtained by de Boer *et al.* (1972) for the coronal condensation from the observed continuum intensity. The value refers to $\rho = 1.02$, ρ being the distance from the solar centre in units of the solar radius. The ionization equilibrium calculations of Landini & Fossi indicate that the temperature of 2.5×10^6 K would be reasonable to account for Ca xv lines in the coronal condensation. In table 2 we have listed the difference between the observed and theoretical line intensity ratios for the four sets of the physical parameters.

Table 2. The difference between the observed and theoretical line intensity ratios : $\log (R^{\text{obs}}/R^{\text{theo}})**$

Ions	$N_e = 5 \times 10^8 \text{ cm}^{-3}$					$N_e = 7.5 \times 10^8 \text{ cm}^{-3}$				
	$1.0 \times 10^6 \text{ K}$	$2.5 \times 10^6 \text{ K}$	$1.25 \times 10^6 \text{ K}$	$2.5 \times 10^6 \text{ K}$	$1.0 \times 10^6 \text{ K}$	$2.5 \times 10^6 \text{ K}$	$1.25 \times 10^6 \text{ K}$	$2.5 \times 10^6 \text{ K}$	$1.0 \times 10^6 \text{ K}$	$2.5 \times 10^6 \text{ K}$
Ca xv ^a /Ca xii		0.07		0.15		0.15		0.22		0.22
Ca xv ^a /Ca xiii		(-0.53)		(-0.52)		(-0.49)		(-0.49)		(-0.49)
Ca xiii/Ca xii		0.10		0.10		0.07		0.07		0.07
		(0.70)		(0.77)		(0.70)		(0.77)		(0.77)
Ca xv ^a /Fe xiv		-0.82		-0.74		-0.76		-0.68		-0.68
Ca xiii/Fe xiv		-0.88		-0.89		-0.90		-0.90		-0.90
Ca xii/Fe xiv	-0.88	-0.88	-0.89	-0.89	-0.96	-0.90	-0.91	-0.90	-0.90	-0.90
Ca xiii/Fe xi ^a		-1.10		-0.83		-0.85		-0.56		-0.59
Ca xiii/Fe xi ^b		-1.11*		-0.84*		-1.14*		-0.82*		-0.81*
Ca xii/Fe xi ^a	-1.11	-1.04	-0.83	-0.86	-1.10	-0.85	-0.81	-0.59	-0.81*	-0.59
Ca xii/Fe xi ^b	-1.13*	-1.11*	-0.84*	-0.81*	-1.11*	-1.14*	-0.82*	-0.81*	-0.81*	-0.81*
Ca xii/Fe x	-0.66	-0.67	-0.78	-0.76	-0.68	-0.67	-0.80	-0.77	-0.77	-0.77
Fe xi ^b /Fe xiv	0.23	0.20	-0.05	-0.02	0.19	-0.05	-0.09	-0.31	-0.31	-0.31
Fe xi ^b /Fe xiv	0.25*	0.22*	-0.05*	-0.07*	0.21*	0.24	-0.09*	0.09*	0.09*	0.09*
Fe xi ^a /Fe x	0.45	0.42	0.06	0.10	0.41	0.18	0.02	-0.18	-0.18	-0.18
Fe xi ^b /Fe x	0.47*	0.44*	0.06*	0.05*	0.40*	0.47*	0.03*	0.05*	0.05*	0.05*
Fe x/Fe xiv	-0.22	-0.22	-0.11	-0.13	-0.22	-0.23	-0.11	-0.14	-0.14	-0.14

Notes : Values within brackets are by using actual observed intensities.

*Values obtained using estimated line intensities

** $I(i) =$ intensity in the line i ; $I(j) =$ intensity in the line j ; $R = I(i)/I(j)$; $R^{\text{obs}} =$ observed ratio; $R^{\text{theo}} =$ theoretical ratio.

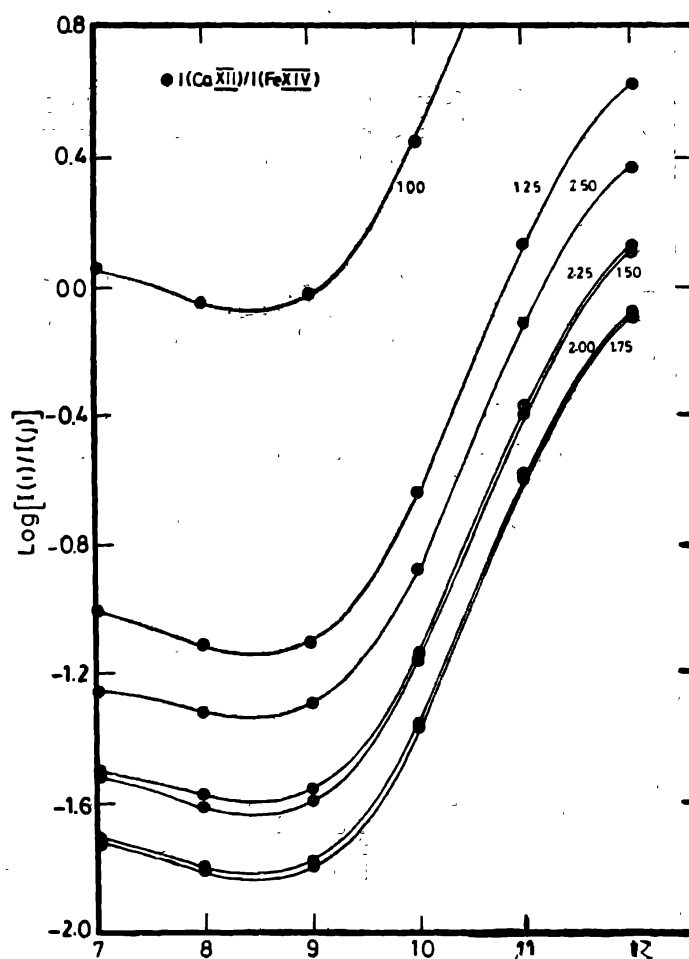


Figure 5. Same as for figure 1.

$I(i)$ defines the intensity for the line i and $I(j)$ for the line j . R defines the intensity ratio for the two lines. In table 2 we have not considered the infrared lines of Fe XIII. The emission line intensities listed by de Boer *et al.* (1972) for the coronal condensation are restricted to the wavelength range $\lambda\lambda 3000-9000\text{\AA}$. However, infrared lines of Fe XIII have been observed on a few occasions (Noëns *et al.* 1984). Column one of the table 2 defines the respective ions for the two lines. To obtain the various intensity ratios we need to know the contribution to the total intensity from the two different temperature zones. For instance, Fe XIV line could have reasonable contribution at 1.25×10^6 K. With the help of tabulated emissivities at various temperatures we could obtain the individual contributions from the two temperature layers.

Columns 2, 3, 4 and 5 contain the differences between the observed and theoretical intensity ratios at four electron temperatures, electron density being $5 \times 10^8 \text{ cm}^{-3}$. Similarly columns 6, 7, 8 and 9 contain the differences for electron density of $7.5 \times 10^8 \text{ cm}^{-3}$. The gaps in the table are due to the fact that the emissivities at the lower or the higher temperature are insignificant to be considered.

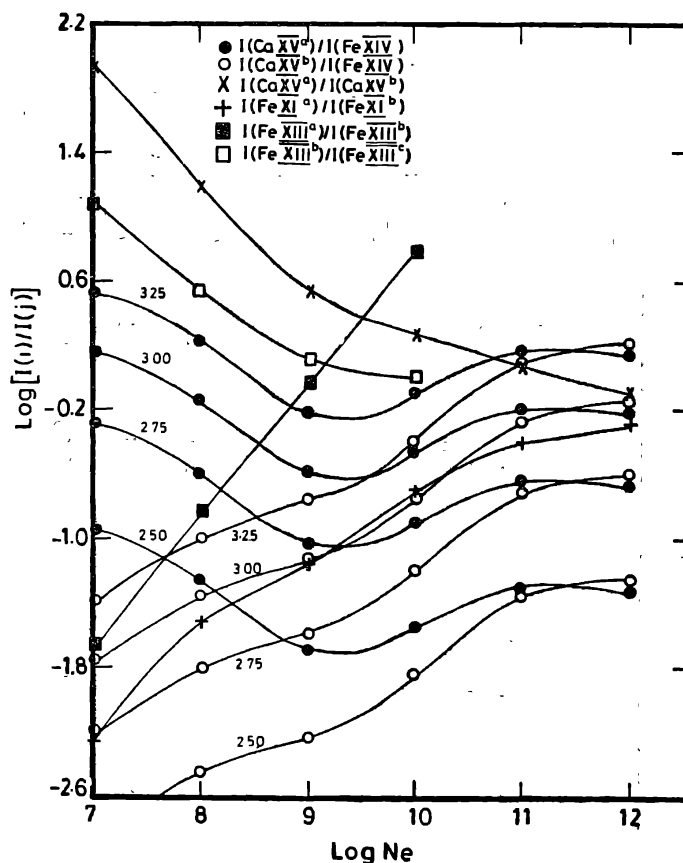


Figure 6. Same as for figure 1.

The theoretical ratios used in table 2 have been calculated taking the relative abundance of Ca to Fe to be 8.5×10^{-2} (Mason 1975). This relative abundance is 3.4 times larger than the value obtained by de Boer *et al.* (1972). Assuming that the value used by Mason is large, we can reduce the difference between the observed and theoretical ratios for Ca/Fe in table 2. We notice that the agreement between observed and theoretical ratios becomes reasonable when the emitting regions are at 1.25×10^6 K and 2.5×10^6 K with an electron density of 5×10^8 cm $^{-3}$. Any residual discrepancies in the differences of ratios in table 2 could be mainly due to the simplified model and to a lesser extent due to the uncertainties in observed intensities, ionization equilibrium densities, and atomic data.

de Boer *et al.* (1972) in their investigation on coronal abundances use the continuum flux to obtain the total number of electrons in the line of sight for the observed condensation. With this parameter plus the two temperature zones, one at 1.0×10^6 K and the other at 2.5×10^6 K, and a constant electron density of 6×10^8 cm $^{-3}$ they estimated the line intensities in various lines. They are listed in the last column of table 3. For Fe XI line at 7892 Å observed intensity is not available. This intensity was computed from the theoretical ratio with the help of the observed intensity for the Fe XI line at 3986 Å. These ratios in table 2 are indicated by asterisks. The values within the brackets are the ones

Table 3. Estimated line intensities ($\text{erg cm}^{-2} \text{s}^{-1} \text{sterad}^{-1}$)

Ion (λ , \AA)	$T_e \times 10^4 \text{K}$		$N_e : 5 \times 10^8 \text{cm}^{-3}$					$N_e : 7.5 \times 10^8 \text{cm}^{-3}$					de Boer <i>et al.</i> (1972)	
	1.0	2.5	1.0	1.25	2.5	1.0	1.25	2.5	1.0	1.25	2.5			
Ca xv (5694)	—	0.21	—	—	0.21	—	—	—	—	—	0.21	—	—	—
Ca xv (5445)	—	0.036	—	—	0.030	—	—	—	—	—	0.031	—	—	—
Ca xiii (4088)	—	0.42	—	—	0.35	—	—	—	—	—	0.32	—	—	(1.65 : observed)
Ca xii (3327)	0.03	0.33	0.03	0.09	0.27	0.03	0.09	0.33	0.03	0.09	0.27	0.09	0.09	0.40*
Fe xiv (5303)	0.28	54.62	0.28	9.2	45.7	0.28	54.62	54.62	0.28	9.2	45.7	9.2	45.7	(0.36 : observed)
Fe xiii (3388)														370*
Fe xiii (10747)														(54.9 : observed)
Fe xiii (10797)														21*
Fe xi (3987)	4.03	0.02	4.03	4.04	0.01	4.05	—	—	4.05	4.05	—	—	—	(16.1 : observed)
Fe xi (7892)	72.7	0.2	72.7	72.8	0.10	63.3	0.3	0.3	63.3	63.5	0.1	0.1	0.1	95*
Fe x (6374)	60.38	0.02	60.38	60.38	0.02	60.38	0.02	0.02	60.38	60.38	0.02	0.02	0.02	74*
														4.3*
														(4.05 : observed)
														75*
														150*
														(60.4 : observed)

*Line intensities estimated by de Boer *et al.* (1972).

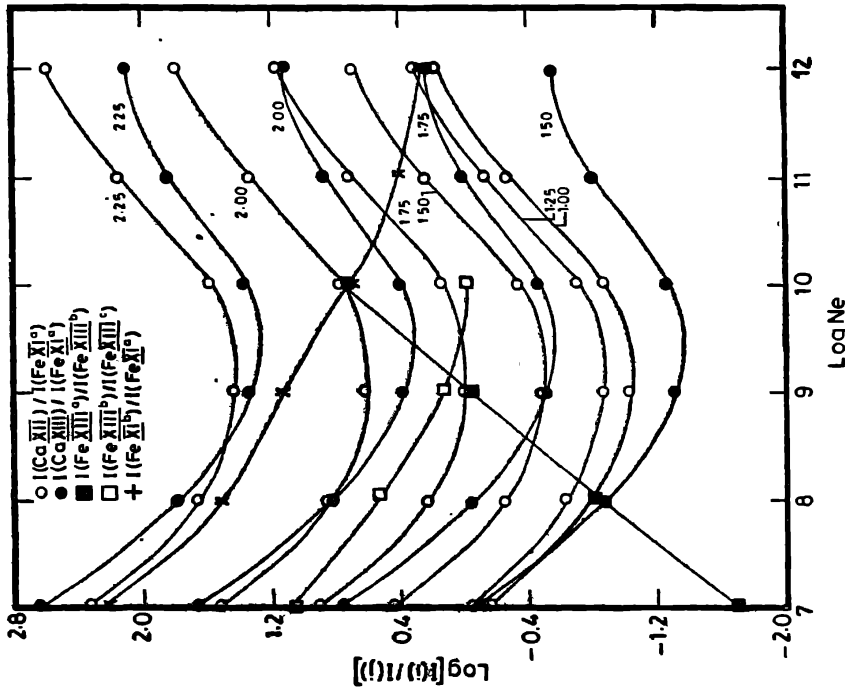


Figure 8. Same as for figure 1.

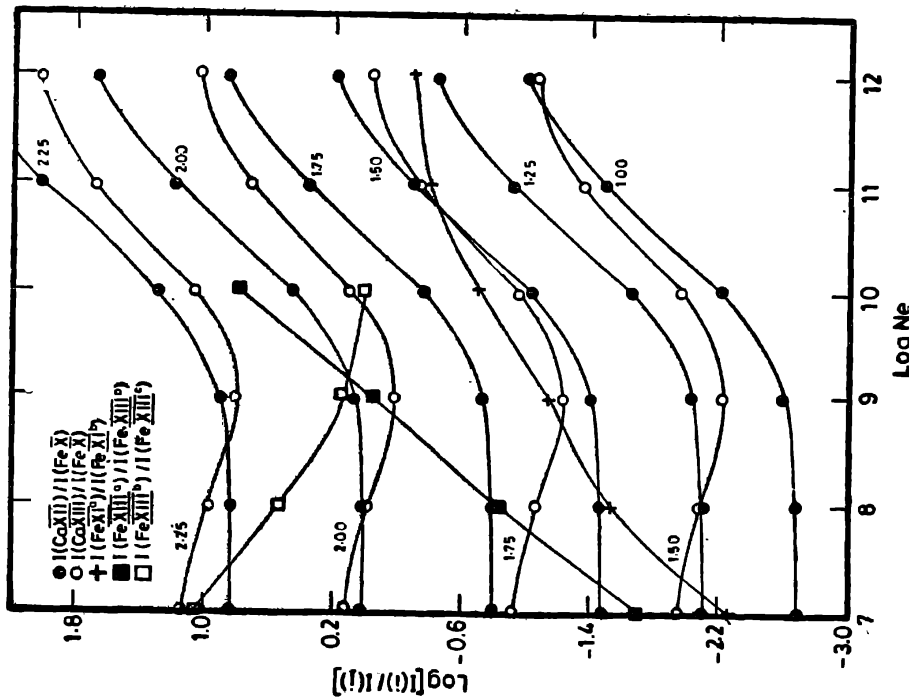


Figure 7. Same as for figure 1.

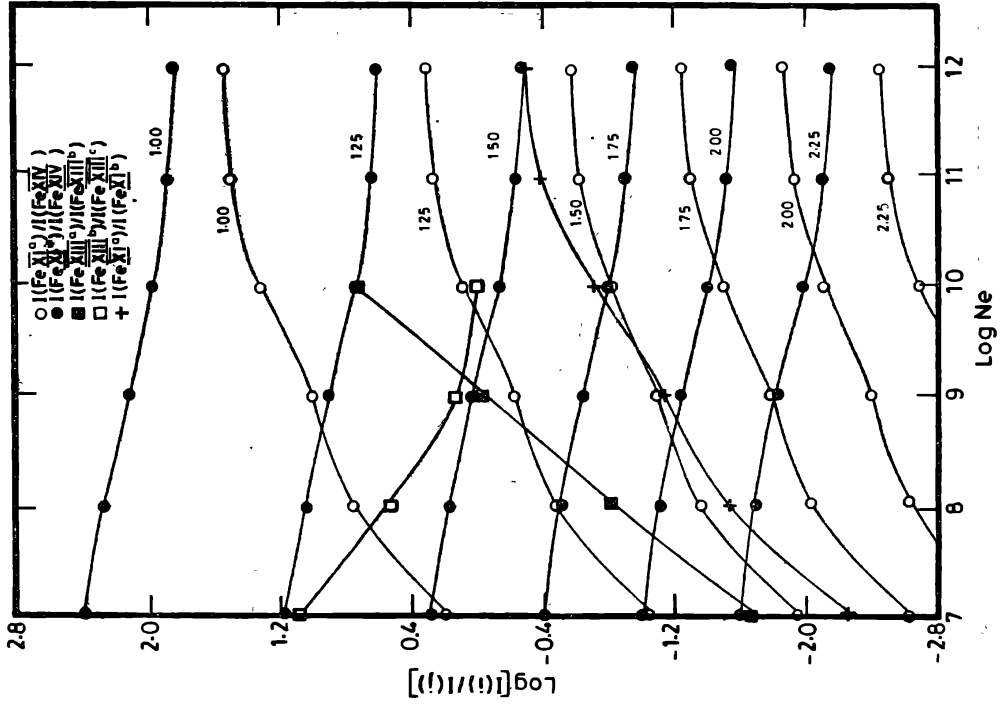


Figure 10. Same as for figure 1.

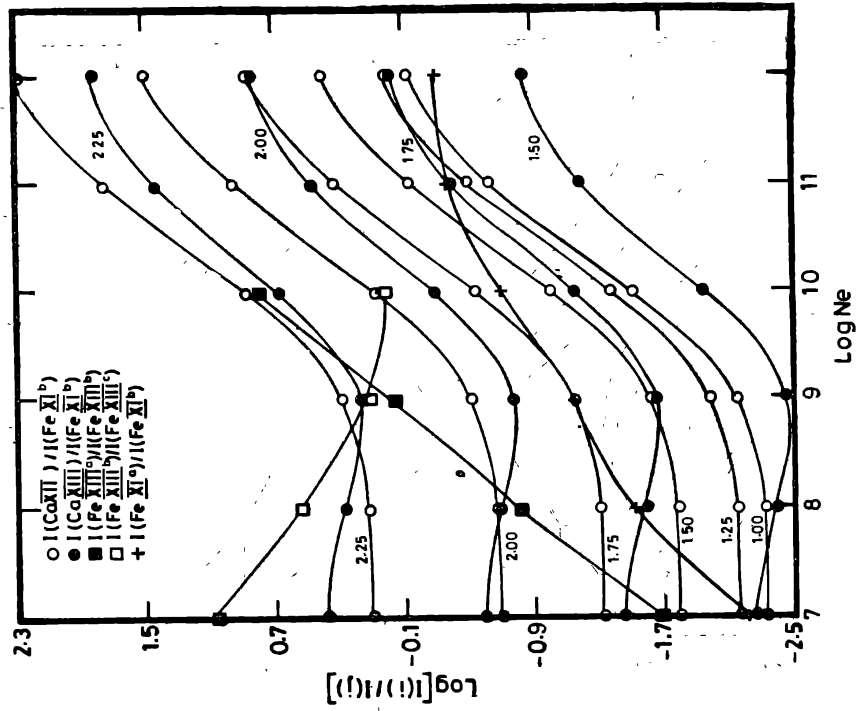


Figure 9. Same as for figure 1.

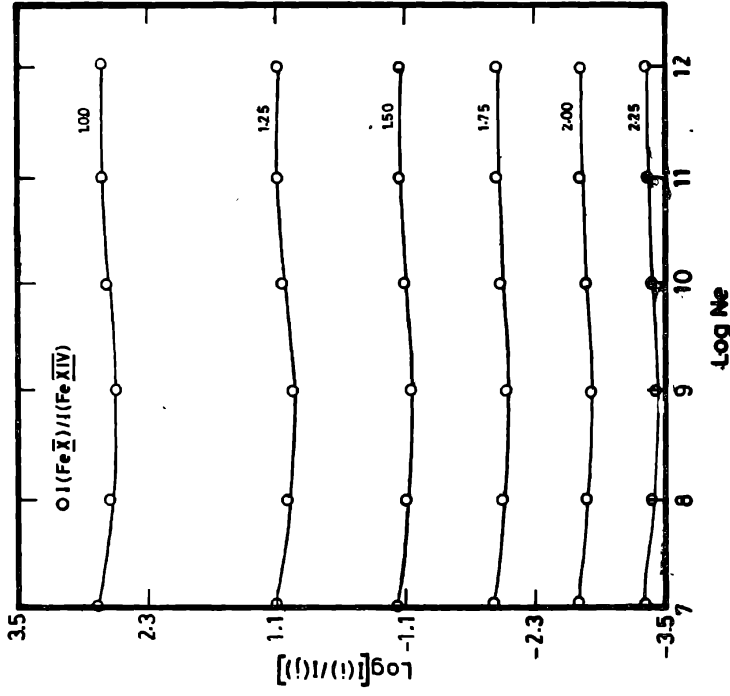


Figure 11. Same as for figure 1.

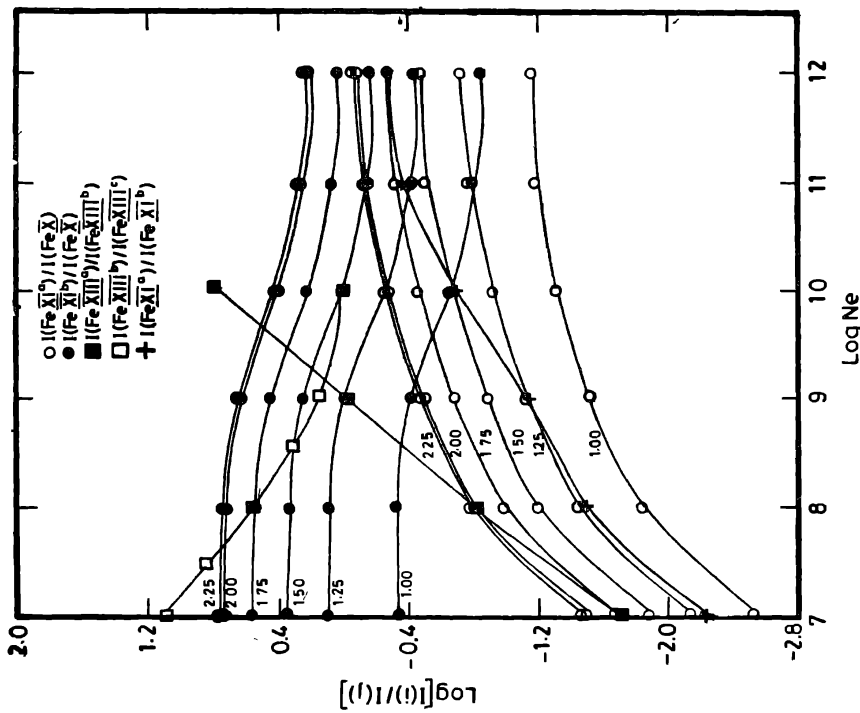


Figure 12. Same as for figure 1.

when we use the observed intensities for Ca lines, allowing for the contributions at the two temperatures. It seems that the observed intensity for Ca XIII line at 4088 Å is large by about a factor of 4. The other ratios in the table 2 were obtained when this correction factor was taken into account. Using the theoretical ratios for Fe XIII line (Flower & Pineau des Forêts 1973) and the observed line intensity for Fe XIII line at 3388 Å we have estimated the intensities for 10747 Å and 10797 Å lines of Fe XIII. These and other estimated intensities are given in table 3.

4. Conclusion

Theoretical line intensity ratios for Ca and Fe coronal ions have been used to infer physical parameters for a coronal condensation. Our analysis indicates that a simple model consisting of two regions of equal path length, one at a temperature of 1.25×10^6 K and the other at 2.5×10^6 K, seems to explain the observed intensities, the electron density of 5×10^8 cm⁻³ being same in both the regions. The procedure adopted suggests that with the availability of reliable line emission rates, theoretical as well as observational, for many more coronal ions it should be possible to construct more realistic models for emission regions. In addition, the analysis outlined above would provide valuable information on relative elemental abundances.

Acknowledgement

I am grateful to the unknown referees whose useful comments have helped in considerably improving the presentation.

References

- de Boer, K. S. Olthof, H. & Pottasch, S. R. (1972) *Astr. Ap.* **16**, 417.
Flower, D. R. & Pineau des Forêts, G. (1973) *Astr. Ap.* **24**, 181.
Landini, M. & Monsignori-Fossi, B. C. (1972) *Astr. Ap. Suppl.* **7**, 291.
Mason, H. E. (1975) *M.N.R.A.S* **170**, 651.
Noëns, J. C., Pageadult, J. & Ratier, G. (1984) *Solar Phys.* **94**, 117.